Surface Exchange and Shape Transitions of PbSe Quantum Dots during Overgrowth

L. Abtin,[1] G. Springholz,[1,*] and V. Holy[2]
[1]Institut für Halbleiter- und Festkörperphysik, Johannes Kepler Universität, A-4040 Linz, Austria
[2]Charles University, Faculty of Mathematics and Physics, Praha, Czech Republic
(Received 7 August 2006; published 28 December 2006)

Epitaxial overgrowth of PbSe quantum dots is shown to drastically affect their shape and composition due to anion exchange reactions. As shown by scanning tunneling microscopy, for PbTe capping layers this results in a complete truncation of the dots. Introduction of EuTe into the cap layer leads to an effective suppression of the anion exchange process. This preserves the original dot pyramids and induces a large stress concentration on the surface which further alters the overgrowth process.

DOI: 10.1103/PhysRevLett.97.266103 PACS numbers: 68.65.Hb, 68.37.Ef, 81.07.Ta, 81.15.Hi

Self-assembled semiconductor quantum dots are of great importance for optoelectronic devices. Their synthesis is based on the Stranski-Krastanow growth mode of lattice-mismatched heteroepitaxy in which three-dimensional (3D) surface nanoislands spontaneously nucleate on a 2D wetting layer to relax the elastic energy of the system [1]. For practical device applications, these dots have to be covered by a protective capping layer in order to suppress surface oxidation as well as nonradiative carrier recombination. Experimental studies have indicated, however, that during this capping process a strong redistribution of the dot material takes place [2–11]. For example, Si capping of Ge nanoislands was found to result in a reverse shape transition from multifaceted domes to pyramids [3,4], and self-assembled InAs dots tend to be transformed into shallow lens- [6–9] or ring-shaped [2,9] structures. This modifies the electronic properties as well.

In this Letter, we focus on the role of the chemical composition of the capping layer on the overgrowth process of self-assembled PbSe quantum dots. Using *in situ* scanning tunneling microscopy, we reveal that an intricate interplay between surface exchange and shape transitions occurs. This strongly depends on the cap layer composition and not only influences the surface evolution but also the final shape and composition of the dots. While for pure PbTe overgrowth, anion exchange leads to a rapid dot dissolution, this is effectively suppressed by the introduction of EuTe into the capping material. Thus, the pyramidal structure of the native PbSe dots is completely preserved. The reduced intermixing induces a high stress concentration on the cap surface such that deep holes and trenches are formed due to repulsion of deposited adatoms. The comparison with theoretical calculations shows that the structure of these trenches exactly mirrors the surface strain distribution and that the trenches are filled up only when the surface stress falls below a critical value.

The samples were grown by molecular beam epitaxy onto PbTe (111) buffer layers [12,13]. Their structures consist of 5 monolayers (ML) PbSe dots followed by $Pb_{1-x}Eu_xTe$ capping layers with composition varying between $x_{Eu} = 0$ and 8% and thicknesses from 10 to 200 Å. Identical growth conditions were used for all samples with a substrate temperature of 350 °C and PbSe and PbEuTe flux rates of 0.12 and 1 ML/sec, respectively. Because of the −5.4% lattice mismatch, PbSe dots are formed at a critical coverage of 1.5 ML, and at 5 ML the surface is uniformly covered by dots with a density of $\sim 250/\mu m^2$. Immediately after growth, the samples were quenched to room temperature and transferred to an attached ultrahigh vacuum scanning tunneling microscopy (STM) chamber. Surface imaging was performed at a sample bias of 1–2 V and selected samples were also characterized by *ex situ* atomic force microscopy.

Figure 1(a) shows the 3D surface image of the initial uncapped PbSe islands, representing the starting condition for the overgrowth experiments. From a statistical analysis, the as-grown dots display an average height of 110 Å and a base width of 205 Å, both with a dispersion of ±12%. All dots exhibit an identical pyramidal shape defined by three low-energy {100} side facets [12,13] and a triangular base aligned along the $\langle \bar{1}10 \rangle$ directions. In the first set of experiments, the dots were capped with PbTe layers and the surface evolution captured by STM. As revealed by Fig. 1, with increasing cap thickness a rapid shrinking of

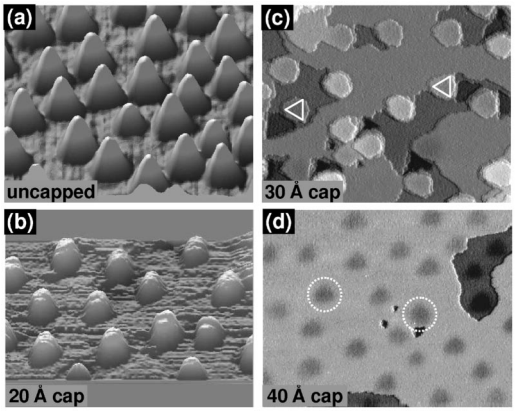

FIG. 1. Surface images ($0.3 \times 0.25\ \mu m^2$) of 5 ML PbSe dots covered with different PbTe cap thicknesses: (a) Uncovered dots. (b)–(d) Cap thickness of 20, 30, and 40 Å, respectively.

dot height and transition in shape occurs. Already after 20 Å PbTe deposition [Fig. 1(b)], the dots are transformed into truncated pyramids and their height is reduced to half of the original value. At 30 Å cap thickness [Fig. 1(c)], the surface has become almost completely flat with just the top 1–3 ML of the pyramid trunks still sticking out through the capping layer. Thus, the whole upper part of the dots has been completely dissolved. The flat top plateaus of the dots show a substantial rounding of the corners and the width has notably increased compared to the original dot pyramids indicated by white triangles in Fig. 1(c). Thus, the dot material has been redistributed towards the island edges. Further incrementing the cap thickness to 40 Å [Fig. 1(d)] renders a completely planarized surface with the usual 200 nm wide monolayer terraces typical for PbTe epilayers [13]. In addition, however, evenly distributed shallow triangular surface depressions appear on these terraces. Their density exactly matches the density of the buried dots and thus, they stem from the local lattice distortions induced by the dots.

A strikingly different surface evolution takes place when the dots are overgrown with $Pb_{0.92}Eu_{0.08}Te$ capping layers. This is demonstrated by the series of STM images displayed in Fig. 2. At 80 Å cap thickness, the PbSe pyramids still stick out through the cap layer [Fig. 2(a)] and their tips remain visible even at 100 Å cap thickness [Fig. 2(b)]. In addition, the apices of the dots clearly retain the triangular shape of the pristine PbSe pyramids as evidenced by the STM images shown as insets. Thus, the native PbSe dots are completely preserved and the deposited capping material just fills up the space between the islands. Although at this stage, the surface between the dots is already rather flat, deep trenches remain at the perimeter of the dots; i.e., the growth is strongly suppressed at the pyramid edges. The peculiar structure of the trenches, revealed by the inset of Fig. 2(b), consists of a 200 Å wide triangular shaped denuded zone around the apex of the dots and additional deep holes at the pyramid corners. The depth of the trenches increases from 2–3 ML at 80 Å cap thickness to 5–8 ML at 100 Å cap thickness. As a result, the apices remain visible even at 120 Å cap thickness that exceeds the original dot height. As growth further proceeds, the trenches eventually merge together and just one single ~10 ML deep hole is left above each island [STM image of Fig. 2(c)]. The corresponding zoomed-in STM image signifies that the inner structure of these holes still displays the triangular symmetry of the original PbSe dots elongated along the $\langle\bar{2}11\rangle$ corner directions. Only after further PbEuTe deposition, the holes start to be filled up such that at 160 Å a completely planar surface is regained [Fig. 2(d)]. On the wide and flat monolayer terraces of this surface again the signature of the buried dots in form of shallow triangular surface depressions appear.

For a quantitative analysis of the overgrowth process, STM surface profiles were measured across the dots along the $[\bar{1}10]$ direction. The results are displayed in Figs. 3(a) and 3(b) for both sets of samples. For the PbTe case, the profiles show a rapid transition from sharp to truncated pyramids within 30 Å cap deposition. For the PbEuTe case, the island tips are preserved up to a cap thickness of 120 Å, and even at 140 Å, the islands still reach to the bottom of the holes. To characterize this behavior, the apparent height h_{ap} of the dots indicated by arrows in Fig. 3 was measured as a function of cap thickness. The values are plotted in Fig. 3(e) for PbTe (●) and PbEuTe (■) capping layers, including also data obtained by AFM (□). As indicated by the solid lines, in both cases, the dot height decreases linearly with increasing cap thickness d. The dependence is described by $h_{ap} = (h_0 - k)d$, where h_0 is the initial dot height and k is a scaling constant that characterizes planarization properties of the growth process. For usual thin

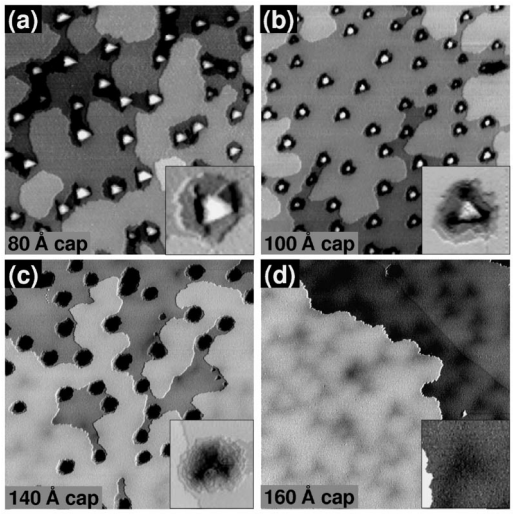

FIG. 2. STM images ($0.5 \times 0.5\ \mu m^2$) of 5 ML PbSe dots covered with $Pb_{0.92}Eu_{0.08}Te$ cap thicknesses of 80, 100, 140, and 160 Å from (a) to (d), respectively. The enlarged images around single dots are shown as insets.

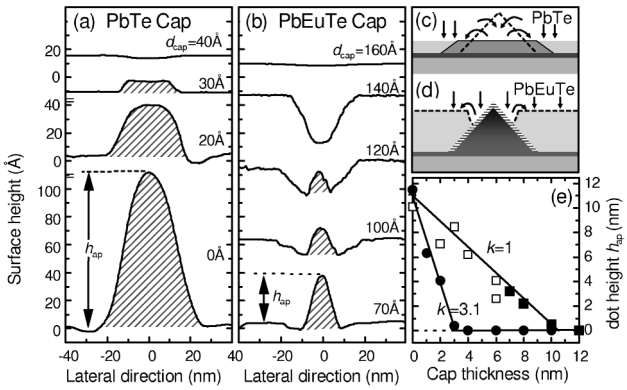

FIG. 3. STM surface profiles across PbSe dots capped with different PbTe (a) or PbEuTe (b) cap thicknesses. The scale is the same for all profiles and the shaded areas indicate the dot part penetrating through the cap surface. (e) Average apparent dot height h_{ap} plotted as a function of PbTe (●) and PbEuTe (■) cap thickness (□: AFM data). The different mechanisms determining the surface evolution are illustrated in (c) and (d).

film deposition, k is generally less than one, with the limiting case of $k = 0$ for conformal overgrowth. For PbEuTe capping, the fit of the experimental data yields a value of $k = 1$, representing the ideal case when growth takes place exclusively in between, but not on top of the islands as shown schematically in Fig. 3(d). For PbTe overgrowth, k exceeds this value by as much as a factor of 3. This signifies that an additional process comes into play that induces a negative growth of the island tops at a rate that is 2 times as large as the deposition rate driven by strong intermixing between the dots and the capping material via anion surface exchange. Generally, intermixing is quite favorable in strained-layer heteroepitaxy because it effectively reduces the lattice mismatch and thus, the total energy of the system. This is because the increase of the volume of strained material induced by intermixing is outweighed by the concomitant reduction of the strain energy per unit volume. The reduced lattice mismatch, on the other hand, reduces the driving force for strain-induced coherent islanding [1]. Therefore, as the Se concentration at the top of the dots is reduced, the material starts to migrate toward the island edges to form more planar surface structures. This is illustrated schematically in Fig. 3(c).

Our model is supported by several control experiments. First of all, we find that PbSeTe ternary layers on PbTe are stable against strain-induced coherent islanding when the Se concentration drops below a critical value of about 40%. Thus, intermixing indeed destabilizes the PbSe dots when the alloying is sufficiently large. Second, the characteristic shape transition is observed only for overgrowth but not during post growth annealing. This indicates that a direct exposure of PbSe with Te atoms is required for the dissolution process. Particular support comes from the dramatic effect of introduction of EuTe into the capping layer. Its role was clarified by an additional set of experiments which showed that predeposition of EuTe layer as thin as 0.2 ML onto the islands before PbTe overgrowth is sufficient to inhibit the dot dissolution process. This proves that atom exchange at the surfaces of the dots is the decisive mechanism for island dissolution. The dramatic effect is explained by the very large difference in binding energy of EuTe compared to the lead salt compounds, where the EuTe value of 7.9 eV per atom pair [14] is nearly twice as large as that for PbSe or PbTe. As a result, the energy barrier for surface exchange is drastically increased.

The consequence for the structure and composition of the buried dots is revealed by analysis of the submonolayer surface depressions observed on the fully planarized cap surfaces. These depressions arise from the elastic lattice distortions around the dots and their amplitude and shape is directly linked to the structure of the buried dots. For a quantitative analysis, line profiles were measured across the surface depressions and averaged over several dots. The results are displayed as solid lines in Figs. 4(c) and 4(d) for 40 Å PbTe and 160 Å PbEuTe cap layers, respectively. To deduce the corresponding dot structure, the surface depressions were modeled assuming coherently strained dots with variable size, shape, and chemical composition. The resulting lattice deformations were calculated using the Fourier method [8]. The PbTe capped dots were modeled as truncated rounded pyramids with a height of $h = 30$ Å, but varying averaged base width b, facet angle α, and composition c_b as shown schematically in Fig. 4(a). The PbEuTe capped dots were modeled as sharp pyramids with {100} facets, a height of 110 Å, and possible vertical gradients in the Se concentration from c_b at the base to c_a in the apex were accounted for [Fig. 4(b)]. From a whole set of calculations we find that the base width and sidewall angle mainly affect the profile shape, whereas the depth mainly depends on the dot composition. This is illustrated by Figs. 4(c) and 4(d), where the profiles calculated for different dot compositions are plotted as dashed lines together with the experimental data, using $b = 340$ Å and $\alpha = 20°$ for PbTe, and $b = 230$ Å and $\alpha = 54°$ for PbEuTe capped dots. For the PbTe case, clearly a good fit is obtained for a Se concentration of 60%, indicating a high degree of Se/Te intermixing. This is attributed partly to intermixing already taking place during the growth of the dots. For the PbEuTe capped dots [Fig. 4(d)], for a good fit the Se content must increase from 83% at the base to 100% at the top. Since the original dot structure is essentially preserved, this gradient must be present already within the uncapped dots. Also from the simulations, the dot width is significantly smaller and the side wall angle much steeper than for PbTe covered dots. This again supports our assertion that for the latter a large amount of material is redistributed toward the island edges.

Knowing the structure of the buried dots, we can clarify the question of why trenches and holes are formed during PbEuTe but not during PbTe overgrowth. For this purpose,

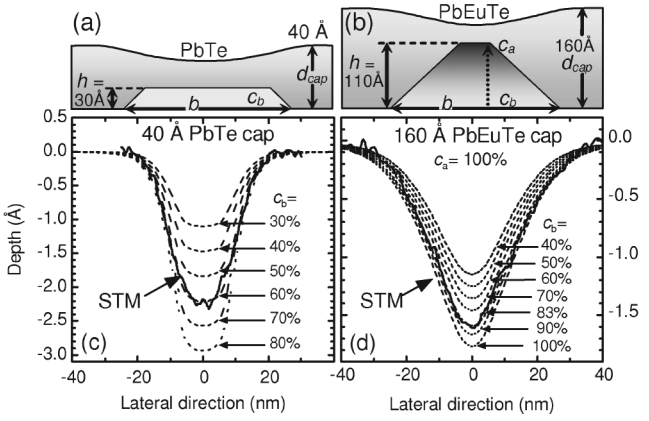

FIG. 4. Top: Buried dot structure used for the elasticity calculations for (a) PbTe and (b) PbEuTe capped dots. Bottom: Averaged STM surface profiles (solid lines) measured over buried dots for (c) 40 Å PbTe and (d) 160 Å PbEuTe cap layers in comparison to surface profiles (dashed lines) calculated for different Se concentrations c. The best fit yields for the PbTe capped dots $c_b = 60\%$, $h = 30$ Å, $b = 340$ Å, and $\alpha = 20°$. For the PbEuTe capped dots $h = 110$ Å, $b = 230$ Å, and $\alpha = 54°$ and c_{Se} increases from 83% at the base to 100% at the top.

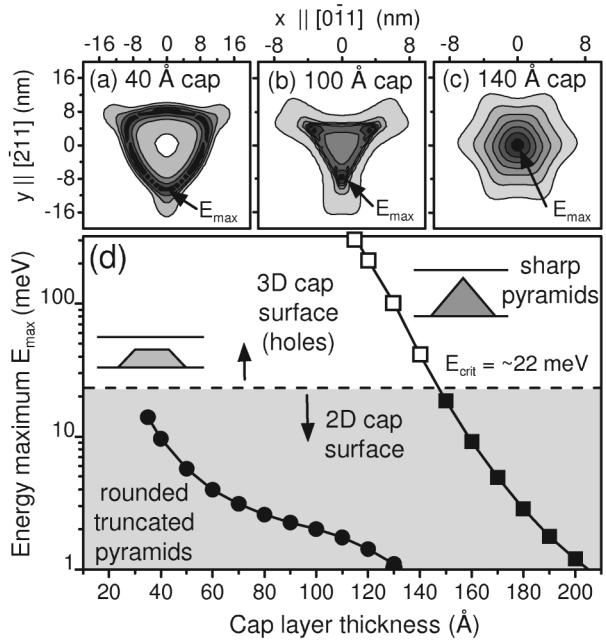

FIG. 5. Surface strain energy distributions on the cap layer calculated for the dot structures derived in Fig. 4: (a) Truncated rounded dot capped with 40 Å PbTe, (b) sharp pyramidal dot capped with 100 Å or (c) 140 Å PbEuTe. Darker colors represent regions of higher strain and the isoenergy contour spacing is 2, 70, and 6 meV/atom pair for (a) to (c), respectively. Bottom: Energy maxima of the strain distribution plotted as a function of PbTe (●) and PbEuTe (■) cap thickness. Open symbols indicate the structures where trenches are observed by STM, solid symbols indicate structures with completely planarized cap layer.

we calculate the strain energy distribution on the surface of the capping layer to assess the stress concentration induced by the buried dots. As input parameters we use the shape and composition of the buried dots obtained above, but we consider only the situation of a fully planar cap surface, noting that the stress concentration will be even enhanced by the trenches at the island edges. Figures 5(a)–5(c) show the calculated surface strain energy distributions for PbTe and PbEuTe cap layers with 40, 100, and 140 Å thickness, respectively. For thin PbTe cap layers, the surface is strained just above the edges of the islands, thus forming a ringlike stress concentrated region. For the 100 Å PbEuTe cap layer [Fig. 5(b)], a triangular shaped stress concentrated region is formed along the pyramid edges with strongly enhanced stresses at the pyramid corners. Strikingly, the energy contour lines mirror the descending step structure within the trenches seen in the STM images [Fig. 2(b)], and the deep holes formed at the pyramid corners are located exactly at the regions of highest stress concentration. As the PbEuTe thickness increases, the gap between the strain maxima closes and a single central strain maximum is formed [see Fig. 5(c)]. Comparing this strain distribution to the structure of the pits in the STM images [Fig. 2(c)], again a striking one-to-one correspondence of the isostrain energy contour lines with the monolayer step structure within the pits appears. For the PbTe cap layers, the absence of trenches is readily explained by comparing the magnitude of the energy maxima plotted in Fig. 5(d) as a function of cap thickness. Evidently, in both cases the stress concentration rapidly decays with increasing cap thickness, but the values for PbEuTe cap layers of up to 440 meV/atom pair are much higher than those for PbTe layers of less than 15 meV. The latter is due to the lower Se concentration as well as the rounding of the pyramid edges. For the 140 Å PbEuTe cap layer where pits are still present on the surface, the strain energy maxima are still as high as 40 meV, whereas at 150 Å the strain energy drops to 20 meV and the pits on the surface disappear. Thus, this value represents the critical strain energy required for repulsion of the deposited adatoms and indeed, for all structures with lower stress concentration no pits or trenches are observed by STM, neither for PbTe nor for PbEuTe capping layers.

In conclusion, overgrowth of PbSe quantum dots induces pronounced shape transformations due to anion surface exchange reactions, leading to a significant shrinking of height as well as rounding of shape. This process can be suppressed by the introduction of a barrier layer by which the pyramidal structure of the native dots is completely preserved. Our results underline the importance of intermixing processes for the structure of the buried dots and demonstrate that the control of the cap layer composition is an effective means for tailoring the structure of quantum dots as required for device applications.

This work was supported by the FWF, the IRON-SFB and GME of Austria, the MSM Research Program No. 0021620834 of the Czech Republic and the SANDiE EU network of excellence.

*Corresponding author.

[1] See, e.g., V. A. Shchukin and D. Bimberg, Rev. Mod. Phys. **71**, 1125 (1999), and references therein.
[2] J. M. García *et al.*, Appl. Phys. Lett. **71**, 2014 (1997).
[3] P. Sutter and M. G. Lagally, Phys. Rev. Lett. **81**, 3471 (1998).
[4] A. Rastelli, M. Kummer, and H. von Känel, Phys. Rev. Lett. **87**, 256101 (2001).
[5] N. Liu *et al.*, Phys. Rev. Lett. **84**, 334 (2000).
[6] B. Lita, R. S. Goldman, J. D. Phillips, and P. K. Battacharya, Appl. Phys. Lett. **75**, 2797 (1999).
[7] D. M. Bruls *et al.*, Appl. Phys. Lett. **82**, 3758 (2003).
[8] J. Stangl, V. Holý, and G. Bauer, Rev. Mod. Phys. **76**, 725 (2004).
[9] P. Offermans *et al.*, Appl. Phys. Lett. **87**, 131902 (2005).
[10] A. Rastelli, E. Müller, and H. Von Känel, Appl. Phys. Lett. **80**, 1438 (2002).
[11] Q. Gong *et al.*, Appl. Phys. Lett. **85**, 5697 (2004).
[12] G. Springholz *et al.*, Science **282**, 734 (1998).
[13] M. Pinczolits *et al.*, Appl. Phys. Lett. **73**, 250 (1998).
[14] E. Kaldis, in *Crystal Growth: Theory and Techniques*, edited by C. H. L. Goodman (Plenum Press, New York, 1974), p. 49.